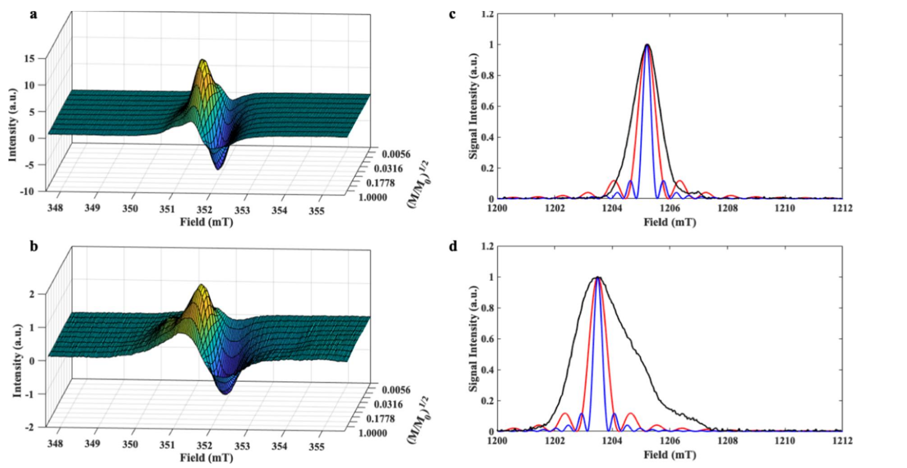

Figure 1. Left panel: (a) X-band (ν = 9.871 GHz) room-temperature power saturation curves of dopa melanin and (b) cysteinyldopa melanin samples. Right panel: EDFS spectra recorded at Q-band (ν = 33.843 GHz) for (c) dopa melanin and (d) cysteinyldopa melanin samples. The red and blue curves in (c) and (d) represent the spectral line shape of the rectangular $\pi/2$ and π pulses, respectively, used to generate the electron spin echo for the EDFS spectra acquisition.

exponential model, $y = A\ \exp\cdot(-t/T_M) + c$, yielding $T_M \approx 262$ ns for the dopa melanin and $T_M \approx 228$ ns for cysteinyldopa melanin samples.

Differences in relaxation times were emphasized when the longitudinal relaxation time (T_1) was measured. T_1 measurements were performed with PFSR experiments to minimize the effect of spectral diffusion.[54] The saturation recovery measurements were performed in the temperature range of 20−110 K (Figure 2). The longitudinal relaxation times were extracted from the saturation curves using the biexponential model $y = A_f{\cdot}\exp(-t/T_{1f}) + A_s{\cdot}\exp(-t/T_{1s}) + c$, which considers the presence of two concurring mechanisms contributing to the longitudinal relaxation process, described by different T_1 values, namely, T_{1f} and T_{1s}. The T_{1f} component is representative of the spectral diffusion effects, and the T_{1s} component is representative of the actual longitudinal relaxation process.

The saturation curves reported in Figure 2a,b show how the saturated magnetization of the melanin pigments is recovered with time from the starting point of the total saturation condition, that is, $\Theta = 1$, to the point of saturation recovery, that is, $\Theta \to 0$.

Together with the data reported in Table 1, Figure 2 depicts the longitudinal relaxation process for the two biomaterials investigated. Faster spin−lattice relaxations were measured for the cysteinyldopa melanin over the entire temperature range. The smaller cysteinyldopa T_{1f} and T_{1s} values can be attributed to the different nature of its radical species. At 40 K (the lowest common temperature investigated for the two pigments), the composed semiquinonimine radical signal of the cysteinyldopa melanin recovered 99% of the equilibrium magnetization level in approximately 2.5×10^{-2} s. The same recovery of the equilibrium magnetization level was reached after approximately 4.5×10^{-2} s in the case of dopa melanin.

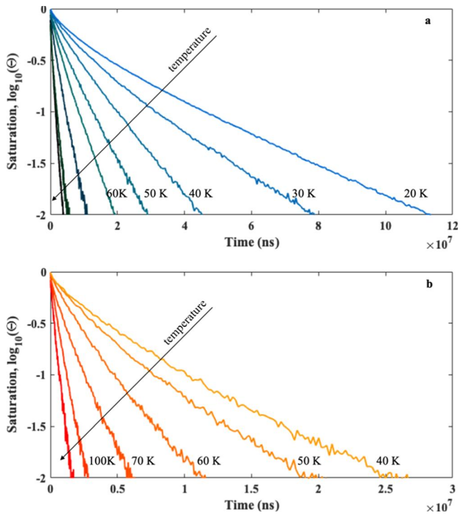

Figure 2. Q-band PFSR curves acquired at variable temperatures for the (a) dopa melanin and (b) cysteinyldopa melanin samples. The $\log_{10}(\Theta)$ represents the saturation recovery process of the macroscopic magnetization in the two samples. The level of saturation percentage is indicated as Θ. The arrow indicates the increasing temperature.

The presence of cysteinyldopa melanin is commonly detected by higher values of the electronic g-factor and by the more complex line shape resolved by CW EPR. Because of the relatively high difference in terms of spin−lattice relaxation

https://dx.doi.org/10.1021/acs.jpcb.9b11785
J. Phys. Chem. B 2020, 124, 2110−2115

Table 1. Longitudinal Relaxation Times[a]

	dopa melanin		cysteinyldopa melanin	
T (K)	T_{1f} (μs)[b]	T_{1s} (μs)[b]	T_{1f} (μs)[b]	T_{1s} (μs)[b]
20	1.15×10^4	6.79×10^4		
30	1.06×10^4	4.90×10^4		
40	5.42×10^3	2.60×10^4	6.07×10^3	2.09×10^4
50	3.93×10^3	1.69×10^4	4.91×10^3	1.69×10^4
60	2.95×10^3	1.12×10^4	2.74×10^3	8.31×10^3
70	2.09×10^3	6.73×10^3	1.94×10^3	5.68×10^3
100	1.53×10^3	4.79×10^3	7.16×10^2	1.90×10^3
110	9.70×10^2	2.66×10^3	4.14×10^2	1.09×10^3

[a]The columns report the T_{1f} and T_{1s} values evaluated for the dopa melanin and cysteinyldopa melanin samples. [b]The error on the reported T_{1f} and T_{1s} values obtained with the biexponential decay model was estimated to be ±3 μs.

times for the two compounds at higher temperature (approaching 60% at 100 K), Q-band PFSR measurements can be proposed as a complementary tool to classic multifrequency CW EPR for the assessment of the nature of new melanin pigments of unknown composition and as an insightful instrument in melanin radical characterization.

Room-temperature PFSR experiments were also performed to assess the measurements of relaxation times as a discriminant feature under common melanin functional conditions (T = 298 K) (Figure 3).

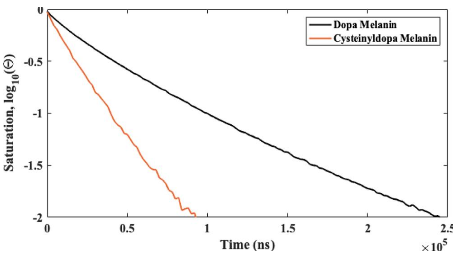

Figure 3. Q-band room temperature (298 K) PFSR curves recorded for dopa melanin (black) and cysteinyldopa melanin (orange). Dopa melanin ν = 33.843 GHz; cysteinyldopa melanin ν = 33.733 GHz.

Figure 3 and Table 2 show that cysteinyldopa faster longitudinal relaxation dynamics point out the feasibility of running T_1 measurement as a discriminant feature for melanin characterization even when EPR room-temperature experiments are considered.

Table 2. Room-Temperature T_{1f} and T_{1s} Values for the Dopa and Cysteinyldopa Melanins

sample	T_{1f} (μs)[a]	T_{1s} (μs)[a]
dopa melanin	61	216
cysteinyldopa melanin	23	58

[a]The error on the reported T_{1f} and T_{1s} values obtained with the biexponential decay model was estimated to be ±3 μs.

Moreover, the T_1 values measured for the dopa melanin produced by laccase (melanin pigments are commonly produced either using tyrosinase or by chemical oxidation of the substrate—tyrosine or dopa) could be compared with those obtained by Okazaki et al., where values of $T_1 \approx 4$ ms were recorded for dopa melanins (77 K), indicating consistency in T_1 values for dopa melanin pigments of different origin.

CONCLUSIONS

This preliminary combined pulse and multifrequency EPR investigation on representative melanins contributes to fill a gap in the rich literature of EPR characterization of melanin pigments.[48] The characterization of the relaxation properties will certainly introduce a new tool to identify and gain information on the pigments, whose structure heterogeneity in the solid state are still the object of intensive research and whose understanding would open up new doors in the biopigment material design.[17]

The same pulse EPR experiments could be extended to other conductive polymers such as polyanilines, where the distribution of relaxation times values could be linked not only to the different polymer chain size but also to a more complex system such as the melanin−polyaniline conductive biopolymers of technological interest.[55−58]

ASSOCIATED CONTENT

Supporting Information

The Supporting Information is available free of charge at https://pubs.acs.org/doi/10.1021/acs.jpcb.9b11785.

X-band CW saturation curves for the dopa melanin and cysteinyldopa melanin, Q-band CW saturation curves for the dopa melanin and cysteinyldopa melanin, and phase memory time measurements for the dopa melanin and cysteinyldopa melanin (PDF)

AUTHOR INFORMATION

Corresponding Author

Rebecca Pogni − *Department of Biotechnology, Chemistry and Pharmacy, Università degli Studi di Siena 53100 Siena, Italy;* orcid.org/0000-0001-6681-1592; Email: rebecca.pogni@unisi.it

Authors

Maher Al Khatib − *Department of Biotechnology, Chemistry and Pharmacy, Università degli Studi di Siena 53100 Siena, Italy*

Jessica Costa − *Department of Biotechnology, Chemistry and Pharmacy, Università degli Studi di Siena 53100 Siena, Italy*

Maria Camilla Baratto − *Department of Biotechnology, Chemistry and Pharmacy, Università degli Studi di Siena 53100 Siena, Italy*

Riccardo Basosi − *Department of Biotechnology, Chemistry and Pharmacy, Università degli Studi di Siena 53100 Siena, Italy*

Complete contact information is available at: https://pubs.acs.org/10.1021/acs.jpcb.9b11785

Notes

The authors declare no competing financial interest.

ACKNOWLEDGMENTS

CSGI (Consorzio per lo Sviluppo dei Sistemi a Grande Interfase), Florence, Italy and MIUR for the Dipartimento di Eccellenza 2018−2022 grant are gratefully acknowledged.

REFERENCES

(1) Wang, Y.; Wang, X.; Li, T.; Ma, P.; Zhang, S.; Du, M.; Dong, W.; Xie, Y.; Chen, M. Effects of Melanin on Optical Behavior of Polymer: From Natural Pigment to Materials Applications. *ACS Appl. Mater. Interfaces* **2018**, *10*, 13100−13106.

(2) Nune, M.; Manchineella, S.; Govindaraju, T.; Narayan, K. S. Melanin incorporated electroactive and antioxidant silk fibroin nanofibrous scaffolds for nerve tissue engineering. *Mater. Sci. Eng., C* **2019**, *94*, 17−25.

(3) d'Ischia, M. Melanin-Based Functional Materials. *Int. J. Mol. Sci.* **2018**, *19*, 228.

(4) Kim, Y. J.; Wu, W.; Chun, S.-E.; Whitacre, J. F.; Bettinger, C. J. Catechol-Mediated Reversible Binding of Multivalent Cations in Eumelanin Half-Cells. *Adv. Mater.* **2014**, *26*, 6572−6579.

(5) d'Ischia, M.; Napolitano, A.; Ball, V.; Chen, C. T.; Buehler, M. J. Polydopamine and Eumelanin: From Structure-Property Relationships to a Unified Tailoring Strategy. *Acc. Chem. Res.* **2014**, *47*, 3541−3550.

(6) Migliaccio, L.; Manini, P.; Altamura, D.; Giannini, C.; Tassini, P.; Maglione, M. G.; Minarini, C.; Pezzella, A. Evidence of Unprecedented High Electronic Conductivity in Mammalian Pigment Based Eumelanin Thin Films after Thermal Annealing in Vacuum. *Front. Chem.* **2019**, *7*, 162.

(7) Di Capua, R.; Gargiulo, V.; Alfè, M.; De Luca, G. M.; Skála, T.; Mali, G.; Pezzella, A. Eumelanin Graphene-like Integration: The Impact on Physical Properties and Electrical Conductivity. *Front. Chem.* **2019**, *7*, 121.

(8) Eom, T.; Woo, K.; Cho, W.; Heo, J. E.; Jang, D.; Shin, J. I.; Martin, D. C.; Wie, J. J.; Shim, B. S. Nanoarchitecturing of Natural Melanin Nanospheres by Layer-by-Layer Assembly: Macroscale Anti-Inflammatory Conductive Coatings with Optoelectronic Tunability. *Biomacromolecules* **2017**, *18*, 1908−1917.

(9) d'Ischia, M.; Napolitano, A.; Pezzella, A.; Meredith, P.; Sarna, T. Chemical and Structural Diversity in Eumelanins: Unexplored Bio-Optoelectronic Materials. *Angew. Chem., Int. Ed.* **2009**, *48*, 3914−3921.

(10) Kumar, P.; Di Mauro, E.; Zhang, S.; Pezzella, A.; Soavi, F.; Santato, C.; Cicoira, F. Melanin-Based Flexible Supercapacitors. *J. Mater. Chem. C* **2016**, *4*, 9516−9525.

(11) Goerlitzer, E. S. A.; Klupp Taylor, R. N.; Vogel, N. Bioinspired Photonic Pigments from Colloidal Self-Assembly. *Adv. Mater.* **2018**, *30*, 1706654.

(12) d'Ischia, M.; Wakamatsu, K.; Cicoira, F.; Di Mauro, E.; Garcia-Borron, J. C.; Commo, S.; Galván, I.; Ghanem, G.; Kenzo, K.; Meredith, P.; et al. Melanins and Melanogenesis: From Pigment Cells to Human Health and Technological. *Pigm. Cell Melanoma Res.* **2015**, *28*, 520−544.

(13) d'Ischia, M.; Wakamatsu, K.; Napolitano, A.; Briganti, S.; Garcia-Borron, J. C.; Kovacs, D.; Meredith, P.; Pezzella, A.; Picardo, M.; Sarna, T.; et al. Melanins and Melanogenesis: Methods, Standards, Protocols. *Pigm. Cell Melanoma Res.* **2013**, *26*, 616−633.

(14) Lopiano, L.; Chiesa, M.; Digilio, G.; Giraudo, S.; Bergamasco, B.; Torre, E.; Fasano, M. Q-Band EPR Investigations of Neuromelanin in Control and Parkinson's Disease Patients. *Biochim. Biophys. Acta, Mol. Basis Dis.* **2000**, *1500*, 306−312.

(15) Kautz, R.; Ordinario, D. D.; Tyagi, V.; Patel, P.; Nguyen, T. N.; Gorodetsky, A. A. Cephalopod-Derived Biopolymers for Ionic and Protonic Transistors. *Adv. Mater.* **2018**, *30*, 1704917.

(16) Amdursky, N.; Głowacki, E. D.; Meredith, P. Macroscale Biomolecular Electronics and Ionics. *Adv. Mater.* **2019**, *31*, 1802221.

(17) Jeong, Y. K.; Park, S. H.; Choi, J. W. Mussel-Inspired Coating and Adhesion for Rechargeable Batteries: A Review. *ACS Appl. Mater. Interfaces* **2018**, *10*, 7562−7573.

(18) Solano, F. Melanin and Melanin-Related Polymers as Materials with Biomedical and Biotechnological Applications— Cuttlefish Ink and Mussel Foot Proteins as Inspired Biomolecules. *Int. J. Mol. Sci.* **2017**, *18*, 1561.

(19) Mostert, A. B.; Powell, B. J.; Pratt, F. L.; Hanson, G. R.; Sarna, T.; Gentle, I. R.; Meredith, P. Role of Semiconductivity and Ion Transport in the Electrical Conduction of Melanin. *Proc. Natl. Acad. Sci. U.S.A.* **2012**, *109*, 8943−8947.

(20) Nawaz, M.; Khan, H. M. S.; Akhtar, N.; Jamshed, T.; Qaiser, R.; Shoukat, H.; Farooq, M. Photodamage and Photoprotection: An In vivo Approach Using Noninvasive Probes. *Photochem. Photobiol.* **2019**, *95*, 1243−1248.

(21) Jakubiak, P.; Lack, F.; Thun, J.; Urtti, A.; Alvarez-Sánchez, R. Influence of Melanin Characteristics on Drug Binding Properties. *Mol. Pharm.* **2019**, *16*, 2549−2556.

(22) Maher, S.; Mahmoud, M.; Rizk, M.; Kalil, H. Synthetic Melanin Nanoparticles as Peroxynitrite Scavengers, Photothermal Anticancer and Heavy Metals Removal Platforms. *Environ. Sci. Pollut. Res.* **2019**, DOI: 10.1007/s11356-019-05111-3.

(23) Mostert, A. B.; Rienecker, S. B.; Noble, C.; Hanson, G. R.; Meredith, P. The Photoreactive Free Radical in Eumelanin. *Sci. Adv.* **2018**, *4*, No. eaaq1293.

(24) Brunetti, A.; Arciuli, M.; Triggiani, L.; Sallustio, F.; Gallone, A.; Tommasi, R. Do Thermal Treatments Influence the Ultrafast Opto-Thermal Processes of Eumelanin? *Eur. Biophys. J.* **2019**, *48*, 153−160.

(25) Ito, S. Reexamination of the Structure of Eumelanin. *Biochim. Biophys. Acta, Gen. Subj.* **1986**, *883*, 155−161.

(26) Godechal, Q.; Ghanem, G. E.; Cook, M. G.; Gallez, B. Electron Paramagnetic Resonance Spectrometry and Imaging in Melanomas: Comparison between Pigmented and Nonpigmented Human Malignant Melanomas. *Mol. Imaging* **2013**, *12*, 218−223.

(27) Godechal, Q.; Leveque, P.; Marot, L.; Baurain, J.-F.; Gallez, B. Optimization of Electron Paramagnetic Resonance Imaging for Visualization of Human Skin Melanoma in Various Stages of Invasion. *Exp. Dermatol.* **2012**, *21*, 341−346.

(28) Xiao, M.; Li, Y.; Allen, M. C.; Deheyn, D. D.; Yue, X.; Zhao, J.; Gianneschi, N. C.; Shawkey, M. D.; Dhinojwala, A. Bio-Inspired Structural Colors Produced via Self-Assembly of Synthetic Melanin Nanoparticles. *ACS Nano* **2015**, *9*, 5454−5460.

(29) Iwasaki, T.; Tamai, Y.; Yamamoto, M.; Taniguchi, T.; Kishikawa, K.; Kohri, M. Melanin Precursor Influence on Structural Colors from Artificial Melanin Particles: PolyDOPA, Polydopamine, and Polynorepinephrine. *Langmuir* **2018**, *34*, 11814−11821.

(30) Capecchi, E.; Piccinino, D.; Bizzarri, B. M.; Avitabile, D.; Pelosi, C.; Colantonio, C.; Calabrò, G.; Saladino, R. Enzyme-Lignin Nanocapsules Are Sustainable Catalysts and Vehicles for the Preparation of Unique Polyvalent Bioinks. *Biomacromolecules* **2019**, *20*, 1975−1988.

(31) Isapour, G.; Lattuada, M. Bioinspired Stimuli-Responsive Color-Changing Systems. *Adv. Mater.* **2018**, *30*, 1707069.

(32) Kolle, M.; Lee, S. Progress and Opportunities in Soft Photonics and Biologically Inspired Optics. *Adv. Mater.* **2018**, *30*, 1702669.

(33) Chen, C.-T.; Chuang, C.; Cao, J.; Ball, V.; Ruch, D.; Buehler, M. J. Excitonic Effects from Geometric Order and Disorder Explain Broadband Optical Absorption in Eumelanin. *Nat. Commun.* **2014**, *5*, 3859.

(34) Roy, S.; Rhim, J.-W. Preparation of Carrageenan-Based Functional Nanocomposite Films Incorporated with Melanin Nanoparticles. *Colloids Surf., B* **2019**, *176*, 317−324.

(35) Ribera, J.; Panzarasa, G.; Stobbe, A.; Osypova, A.; Rupper, P.; Klose, D.; Schwarze, F. W. M. R. Scalable Biosynthesis of Melanin by the Basidiomycete Armillaria Cepistipes. *J. Agric. Food Chem.* **2019**, *67*, 132−139.

(36) Paulin, J. V.; Batagin-Neto, A.; Graeff, C. F. O. Identification of Common Resonant Lines in the EPR Spectra of Melanins. *J. Phys. Chem. B* **2019**, *123*, 1248−1255.

(37) Desmet, C. M.; Danhier, P.; Acciardo, S.; Levêque, P.; Gallez, B. Towards in Vivo Melanin Radicals Detection in Melanomas by Electron Paramagnetic Resonance (EPR) Spectroscopy: A Proof-of-Concept Study. *Free Radical Res.* **2019**, *53*, 405−410.

(38) Kaxiras, E.; Tsolakidis, A.; Zonios, G.; Meng, S. Structural Model of Eumelanin. *Phys. Rev. Lett.* **2006**, *97*, 218102.

(39) Ito, S. A Chemist's View of Melanogenesis. *Pigm. Cell Res.* **2003**, *16*, 230−236.

(40) Plonka, P. M. Electron Paramagnetic Resonance as a Unique Tool for Skin and Hair Research. *Exp. Dermatol.* **2009**, *18*, 472−484.
(41) Zdybel, M.; Pilawa, B.; Drewnowska, J. M.; Swiecicka, I. Comparative EPR Studies of Free Radicals in Melanin Synthesized by Bacillus Weihenstephanensis Soil Strains. *Chem. Phys. Lett.* **2017**, *679*, 185−192.
(42) Commoner, B.; Townsend, J.; Pake, G. E. Free Radicals in Biological Materials. *Nature* **1954**, *174*, 689−691.
(43) Chen, C.-T.; Buehler, M. J. Polydopamine and Eumelanin Models in Various Oxidation States. *Phys. Chem. Chem. Phys.* **2018**, *20*, 28135−28143.
(44) Panzella, L.; Leone, L.; Greco, G.; Vitiello, G.; D'Errico, G.; Napolitano, A.; d'Ischia, M. Red Human Hair Pheomelanin Is a Potent Pro-Oxidant Mediating UV-Independent Contributory Mechanisms of Melanomagenesis. *Pigm. Cell Melanoma Res.* **2014**, *27*, 244−252.
(45) Solano, F. Melanins: Skin Pigments and Much More—Types, Structural Models, Biological Functions, and Formation Routes. *New J. Sci.* **2014**, *2014*, 1−28.
(46) Sarna, T.; Swartz, A. H. The Physical Properties of Melanins. *The Pigmentary System: Physiology and Pathophysiology*, 2nd ed.; Blackwell Publishing Ltd., 2006; pp 311−341.
(47) Kim, Y. J.; Khetan, A.; Wu, W.; Chun, S.-E.; Viswanathan, V.; Whitacre, J. F.; Bettinger, C. J. Evidence of Porphyrin-Like Structures in Natural Melanin Pigments Using Electrochemical Fingerprinting. *Adv. Mater.* **2016**, *28*, 3173−3180.
(48) Okazaki, M.; Kuwata, K.; Miki, Y.; Shiga, S.; Shiga, T. Electron spin relaxation of synthetic melanin and melanin-containing human tissues as studied by electron spin echo and electron spin resonance. *Arch. Biochem. Biophys.* **1985**, *242*, 197−205.
(49) Sarna, T.; Hyde, J. S. Electron Spin-Lattice Relaxation Times of Melanin. *J. Chem. Phys.* **1978**, *69*, 1945−1948.
(50) Mostert, A. B.; Hanson, G. R.; Sarna, T.; Gentle, I. R.; Powell, B. J.; Meredith, P. Hydration-Controlled X-Band EPR Spectroscopy: A Tool for Unravelling the Complexities of the Solid-State Free Radical in Eumelanin. *J. Phys. Chem. B* **2013**, *117*, 4965−4972.
(51) Al Khatib, M.; Harir, M.; Costa, J.; Baratto, M.; Schiavo, I.; Trabalzini, L.; Pollini, S.; Rossolini, G.; Basosi, R.; Pogni, R. Spectroscopic Characterization of Natural Melanin from a *Streptomyces Cyaneofuscatus* Strain and Comparison with Melanin Enzymatically Synthesized by Tyrosinase and Laccase. *Molecules* **2018**, *23*, 1916.
(52) Chikvaidze, E. N.; Partskhaladze, T. M.; Gogoladze, T. V. Electron Spin Resonance (ESR/EPR) of Free Radicals Observed in Human Red Hair: A New, Simple Empirical Method of Determination of Pheomelanin/Eumelanin Ratio in Hair. *Magn. Reson. Chem.* **2014**, *52*, 377−382.
(53) Schweiger, A.; Jeschke, G. *Principles of Pulse Electron Paramagnetic Resonance*; Oxford University Press: Oxford, USA, 2001.
(54) Berliner, L. J.; Eaton, G. R.; Eaton, S. S. Distance Measurements in Biological Systems by EPR. *Biological Magnetic Resonance*; Springer, 2002; Vol. *19*.
(55) Mihai, I.; Addiégo, F.; Del Frari, D.; Bour, J.; Ball, V. Associating Oriented Polyaniline and Eumelanin in a Reactive Layer-by-Layer Manner: Composites with High Electrical Conductivity. *Colloids Surf., A* **2013**, *434*, 118−125.
(56) Grossmann, B.; Heinze, J.; Moll, T.; Palivan, C.; Ivan, S.; Gescheidt, G. Electron Delocalization in One-Electron Oxidized Aniline Oligomers, Paradigms for Polyaniline. A Study by Paramagnetic Resonance in Fluid Solution. *J. Phys. Chem. B* **2004**, *108*, 4669−4672.
(57) Magon, C. J.; De Souza, R. R.; Costa-Filho, A. J.; Vidoto, E. A.; Faria, R. M.; Nascimento, O. R. Spin Dynamics Study in Doped Polyaniline by Continuous Wave and Pulsed Electron Paramagnetic Resonance. *J. Chem. Phys.* **2000**, *112*, 2958−2966.
(58) de Salas, F.; Pardo, I.; Salavagione, H. J.; Aza, P.; Amougi, E.; Vind, J.; Martínez, A. T.; Camarero, S. Advanced Synthesis of Conductive Polyaniline Using Laccase as Biocatalyst. *PLoS One* **2016**, *11*, No. e0164958.

Paramagnetism and Relaxation Dynamics in Melanin Biomaterials

Supporting Information

*Maher Al Khatib, Jessica Costa, Maria Camilla Baratto, Riccardo Basosi, and Rebecca Pogni**
Department of Biotechnology, Chemistry and Pharmacy, Via A. Moro 2, 53100 Siena (Italy)

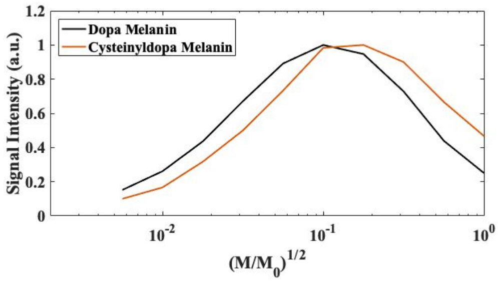

Figure S1 X-band CW saturation curves for the dopa melanin (ν=9.871 GHz) and cysteinyldopa melanin (ν=9.877 GHz). Maximum reference microwave power M_0=144.5 mW

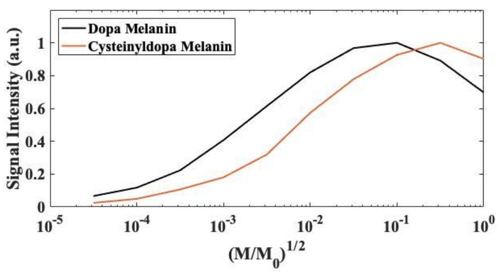

Figure S2 Q-band CW saturation curves for the dopa melanin (ν=33.843 GHz) and cysteinyldopa melanin (ν=33.733 GHz). Maximum reference microwave power M_0=6.3 mW.

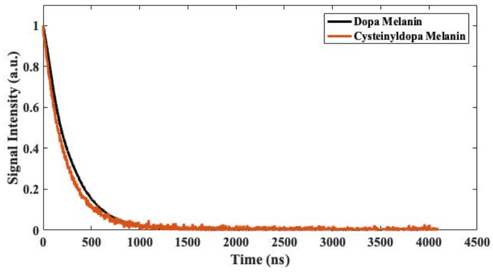

Figure S3 Phase memory time (T_M) measurements for the dopa melanin and cysteinyldopa melanin samples were performed with $\pi/2$-τ-π echo detection sequence with increasing τ values ($\pi/2$=42ns and π=84 ns)